

Supplementary Information

An RNAi nanotherapy for fibrosis: Highly durable knockdown of CTGF/CCN-2 by using siRNA-DegradaBALL (LEM-S401) to treat skin fibrotic diseases

Seounghun Kang^{1†}, Jun Kim^{2†}, Minchul Ahn², Jung-ho Kim², Myeong-Gang Heo², Dal-Hee Min^{1,2*}, and Cheolhee Won^{2*}

¹Department of Chemistry, Seoul National University, Seoul 08826, Republic of Korea.

²Institute of Biotherapeutics Convergence Technology, Lemonex Inc., Seoul 08826, Republic of Korea.

[†]These authors contributed equally.

*To whom correspondence should be addressed: E-mail: dalheemin@snu.ac.kr (D.-H. M.); cheolhee.won@lemonexbio.com (C. W.)

Supplementary figures

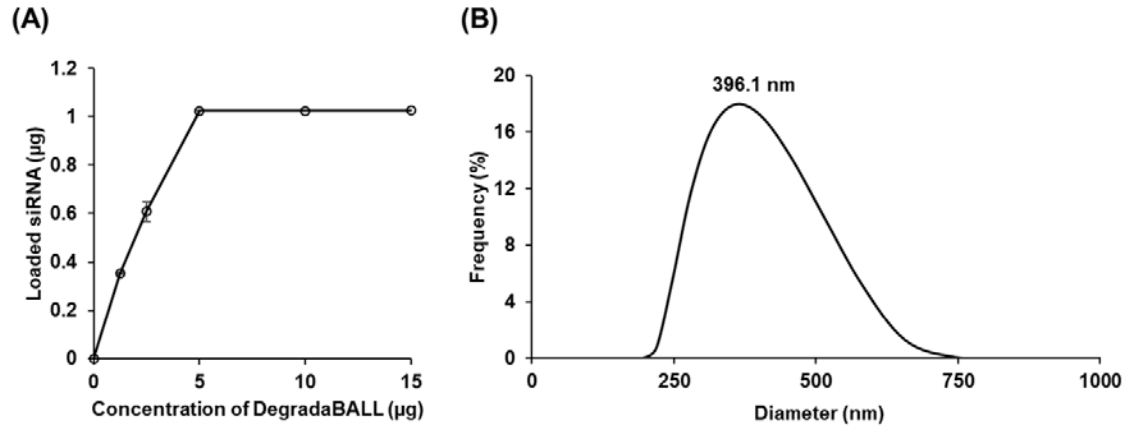


Figure S1. siCTGF loading capacity and dynamic light scattering (DLS) analysis of DegradaBALL. (A) 1 µg of Cy5 conjugated siCTGF was incubated with various concentration of DegradaBALL (0, 1.25, 2.5, 5.0, 10.0 and 15.0 µg). The loaded amount of siCTGF was calculated by fluorescence in the supernatant. (B) DLS analysis of DegradaBALL.

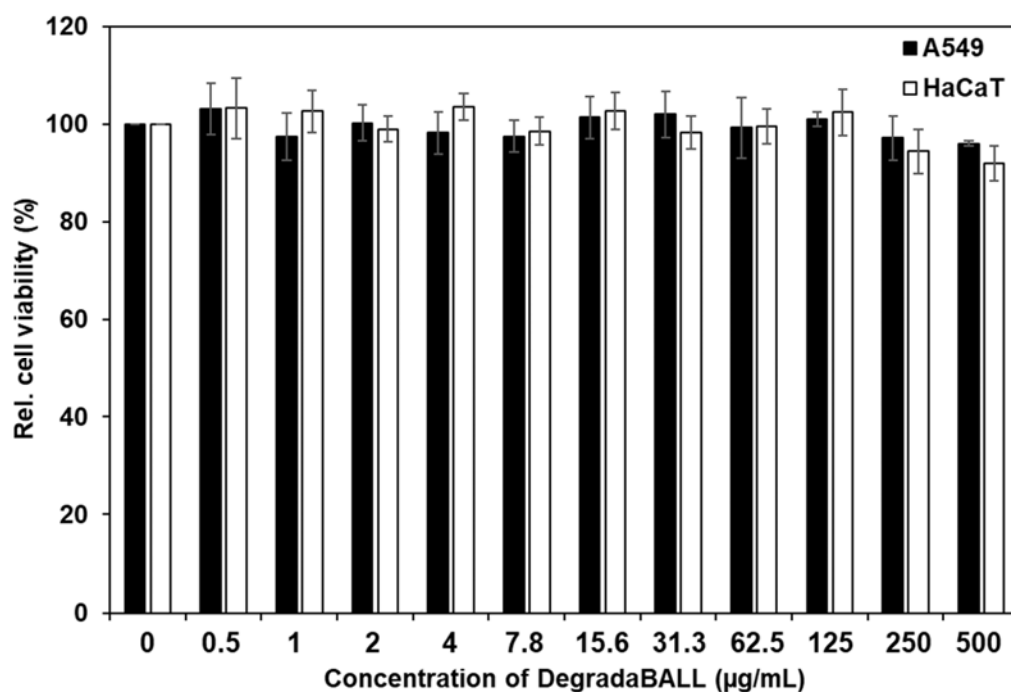


Figure S2. Viability of A549 and HaCaT cells after treatment of DegradaBALL. After treating various doses of DegradaBALL to A549 and HaCaT cells, cell viability was measured by CCK-8 assay.

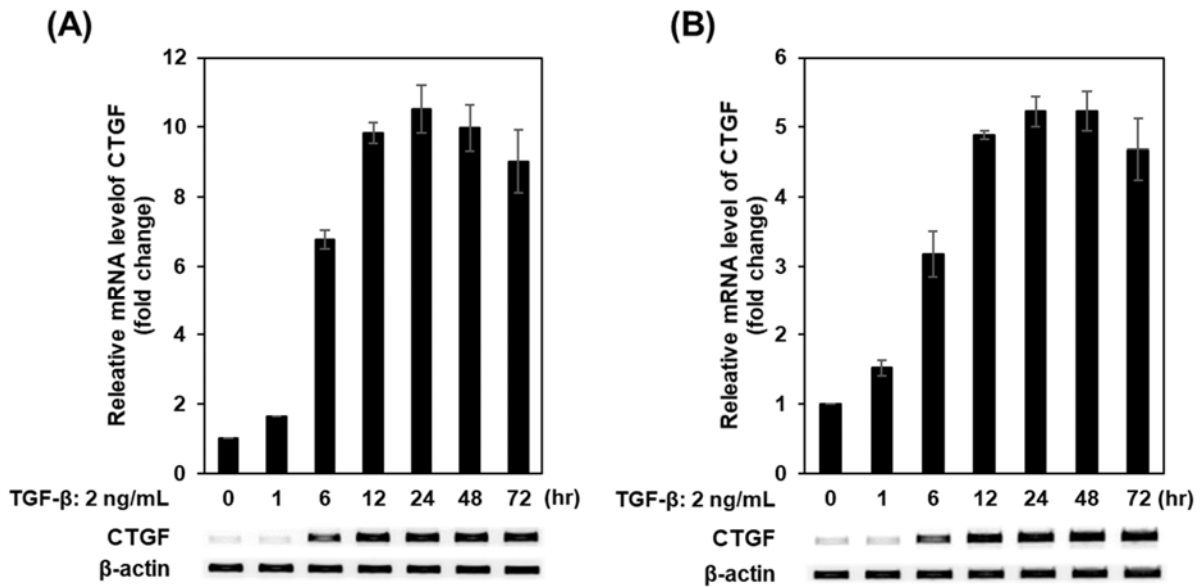
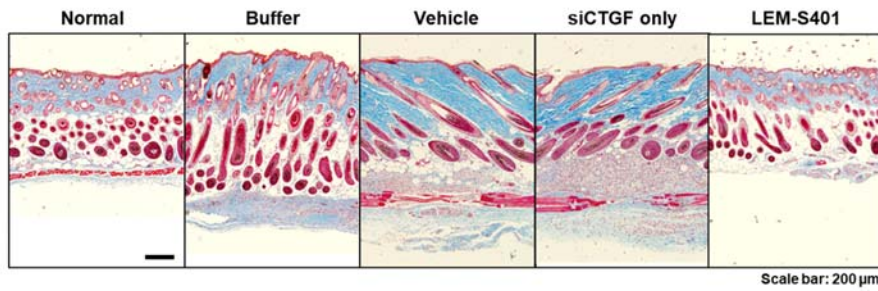
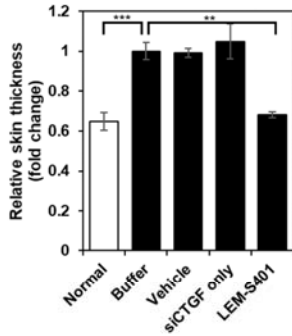


Figure S3. Time-dependent CTGF expression induced by TGF- β . (A) A549 and (B) HaCaT cells were treated with 2 ng/mL of TGF- β for 24 hr. The cells were harvested at different time points and the CTGF expression level was analyzed by RT-PCR.

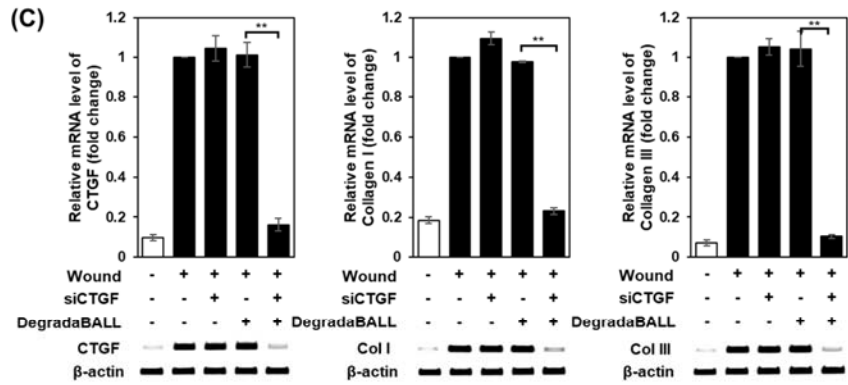
(A)



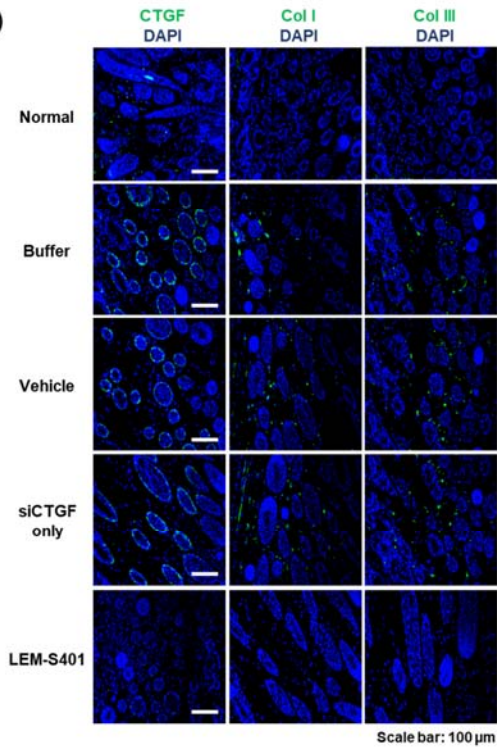
(B)



(C)



(D)



(E)

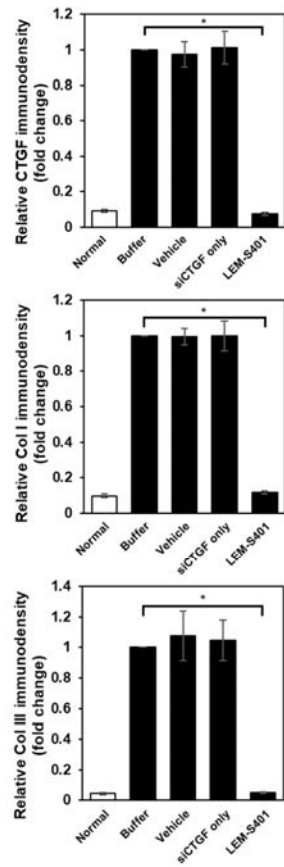


Figure S4. Histopathological photograph of LEM-S401 treated mouse skin during tissue remodeling process in vivo. (A) LEM-S401 was intradermally injected at the wound site on day 10, 14, 18, and 22 post wound formation. The mouse was sacrificed on day 28. (A) the skin tissue was harvested and trichrome stained. (B) Quantitative analysis of skin thickness data based on the images shown in (A). (C) CTGF, Col I and Col III mRNA expression levels in the injection sites were measured by RT-PCR. (D) Fluorescent images of CTGF, Col I and Col III in the harvested mouse skin were examined by immunohistochemistry. Scale bar: 100 μ m. (E) Quantitative analysis of immunohistochemistry data based on the images shown in (D). * P <0.05, ** P <0.01, *** P <0.001

(A)	
Human CTGF siRNA antisense	5'-UCA AGU UCC AGU CUA AUG AG(dTdT)-3'
Human CTGF siRNA sense	5'-CUC AUU AGA CUG GAA CUU GA(dTdT)-3'
Human scramble siRNA antisense	5'-AGC UAA CGU UCA UCU GAA GU(dTdT)-3'
Human scramble siRNA sense	5'-ACU UCA GAU GAA CGU UAG CU(dTdT)-3'
Mouse CTGF siRNA antisense	5'-UAU GUC UUC ACA CUG GUG C(dTdT)-3'
Mouse CTGF siRNA sense	5'-GCA CCA GUG UGA AGA CAU A(dTdT)-3'
(B)	
Human β -actin forward primer	5'-GCT CGT CGA CAA GGG CTC-3'
Human β -actin reverse primer	5'-CAA ACA TGA TCT GGG TCA -3'
Human CTGF forward primer	5'-CAA GGG CCT CTT CTG TGA CT-3'
Human CTGF reverse primer	5'-CCG TCG GTA CAT ACT CCA CA-3'
Mouse β -actin forward primer	5'-GCC TCC CTT CTT GGG TAT GGA A-3'
Mouse β -actin reverse primer	5'-CAG CTC AGT AAC AGT CCG CC-3'
Mouse CTGF forward primer	5'-GGG CCT CTT CTG CGA TTT C-3'
Mouse CTGF reverse primer	5'-ATC CAG GCA AGT GCA TTG GTA-3'
Mouse collagen I forward primer	5'-GAG CGG AGA GTA CTG GAT CG-3'
Mouse collagen I reverse primer	5'-GTT CGG GCT GAT GTA CCA GT-3'
Mouse collagen III forward primer	5'-AGC TTT GTG CAA AGT GGA ACC TGG-3'
Mouse collagen III reverse primer	5'-CAA GGT GGC TGC ATC CCA ATT CAT-3'

Figure S5. Sequence information of siRNA and RT-PCR primers. (A) Human and mouse targeted siRNA sequences. (B) Human and mouse RT-PCR primer sequences.